



Optical Properties of Er³⁺-Yb³⁺ Ions Co-activated Multicomponent Phosphate Glasses for Near-Infrared Applications

M. M. Ismail¹ · I. K. Battisha^{1,2} · D. Geetha³ 

Received: 19 April 2022 / Accepted: 6 December 2022 / Published online: 14 December 2022
© The Author(s) under exclusive licence to Sociedade Brasileira de Física 2022

Abstract

In the present study, Er³⁺-Yb³⁺ co-activated multicomponent phosphate glasses were prepared by conventional melt quenching technique. The x-ray diffraction analysis confirmed the amorphous nature of all the samples. Field emission scanning electron microscopy of the glasses revealed homogeneous and smooth morphology. Moreover, the EDAX results confirmed the existence of phosphate, oxygen, aluminum, sodium, potassium, barium, erbium, and ytterbium in the glass matrix. The optical properties were determined and the absorption coefficient was calculated using absorbance spectrum, which contains 11 bands attributed to the transitions from the ground state ⁴I_{15/2} up to the various higher states ⁴I_{13/2}, ⁴I_{11/2}, ⁴I_{9/2}, ⁴F_{9/2}, ⁴S_{3/2}, ²H_{11/2}, ⁴F_{7/2}, ⁴F_{5/2}, ²G_{9/2}, ⁴G_{11/2}, and ⁴G_{9/2}, respectively. The mentioned bands' presence is due to energy levels reported for Er³⁺ ion glass systems. However, the band around 970 nm is corresponding to ²F_{7/2}→²F_{5/2} (Yb³⁺) and ⁴I_{11/2}→⁴I_{15/2} (Er³⁺) Er³⁺ intra-4F-transition of erbium ions. The radiative properties for the metastable level ⁴I_{13/2} were determined by virtue of the Judd–Ofelt theory. The τ_r slightly decreases with the increase in Yb³⁺ ion sensitizer, and it has maximum value equal to (11.49 ms) for PANBK0.5Er0.5Yb sample. This study introduced promising results to be applied in laser as well as wave guide optical amplifiers' applications around 1.5 μm, with higher intensity emission bands by doping the prepared sample with 0.5 mol% Er³⁺–0.75 mol% Yb³⁺ ions. The PL results in the NIR region at 1.5 μm leading to higher intensity of PANBK0.5Er0.75Yb sample support wave guide optical sensor system application.

Keywords Laser amplifier material · Phosphate glasses · Rare earths · Judd–Ofelt analysis

1 Introduction

Recently, the phosphate glasses have earned widespread attention owing to their interesting applications in optoelectronic devices. Phosphate glasses are inexpensive, highly efficient, and highly transparent and possess long lifetime. Additionally, they are capable of accommodating higher amounts of rare earth and transition metal ions without compromising the optical quality [1]. Rare earth-doped phosphate glasses have been proved to be one of the key optical components as they exhibit interesting spectroscopic

properties [2]. The fluorescence bands exhibited by these glasses in the visible and IR regions attract applications in fiber amplifiers for long-distance communications [3]. Especially Er-doped glasses are competent in overcoming the attenuation constraints in these optical communications [4]. The near-infrared (NIR) emission of the Er³⁺ ions around 1.5 μm, corresponding to ⁴I_{13/2}→⁴I_{15/2} transition, has drawn special interest for telecommunication applications since it is located in the third optical communication window [5, 6]. Activation with Yb³⁺ ions is almost used to enhance the absorption and pumping efficiency of Er³⁺ ions specially in short-length active materials, such as compact laser devices and high-power optical amplifiers devices. The spectral band of the Yb³⁺ ions attributed to ²F_{7/2}→²F_{5/2} transition overlaps with the ⁴I_{15/2}→⁴I_{11/2} transition of Er³⁺ ions, then it is possible to achieve an efficient Yb³⁺ to Er³⁺ ions energy transfer [7, 8]. In the last decade, many active glasses doped with Er³⁺ ions, such as telluride [9], phosphate [10], germanates [11], and fluorides [12], have been investigated. Among all of them, phosphate glasses have the noticeable advantages

✉ D. Geetha
geetha@mitindia.edu

¹ Solid State Physics Department, National Research Centre (NRC), Dokki, 12622 Giza, Egypt

² Electric and dielectric materials measurement Unit, National Research Centre (NRC), Dokki, Giza 12622, Egypt

³ Department of Applied Sciences and Humanities, MIT Campus, Anna University, Chennai-44, India

such as excellent transmission of infrared light, good chemical durability, and thermal stability [13]. Multi-component phosphate glass has the advantage of distinguished network-forming ability and increased rare earth ion solubility, which established it as a promising glass host for high-gain RE-doped fiber [14]. It has also the advantage to increase the rare earth ion solubility in the host multi-component; hence, a higher concentration of optically active ions can be obtained. Its high phonon energy at about (1250 cm^{-1}) is expected to increase the multi-phonon de-excitation probabilities [15], which in the case of Er^{3+} -doped phosphate glass facilitates multi-phonon de-excitation from both the $^4\text{I}_{9/2}$ and $^4\text{I}_{11/2}$ pumping levels of the $^4\text{I}_{13/2}$ emitting level.

In the present study, multi-component phosphate glasses co-activated with Er^{3+} and Yb^{3+} ions were prepared using conventional melt quenching technique. Here Er^{3+} ion concentration is maintained at 0.5 mol% with variable Yb^{3+} ion concentration. The aim is to acquire a better knowledge of the properties of these glasses and thereby improve their efficiency. The structure and spectroscopic properties of the samples analyzed using Judd–Ofelt theory to develop the glass composition and Er–Yb concentrations for wave guide optical amplifier and laser applications.

2 Experimental

2.1 Preparation of the Glasses

Multi component phosphate glasses with the molar composition of $60\% \text{ P}_2\text{O}_5 + 8\% \text{ Al}_2\text{O}_3 + 2\% \text{ Na}_2\text{O} + 13\% \text{ BaO} + (16.5 - x)\% \text{ K}_2\text{O} + 0.5\text{Er}_2\text{O}_3 + X\% \text{ Yb}_2\text{O}_3$, (where $x = 0.5, 0.75, \text{ and } 1\%$), symbolic as PANBK0.5Er0.5Yb, PANBK0.5Er0.75Yb, and PANBK0.5Er1Yb respectively, were prepared using conventional melt-quenching technique. High purity P_2O_5 , Al_2O_3 , Na_2CO_3 , BaCO_3 , K_2CO_3 , $\text{Er}(\text{NO}_3)_3(5\text{H}_2\text{O})$, and $\text{Yb}(\text{NO}_3)_3(5\text{H}_2\text{O})$ were used as starting materials to prepare the mentioned glasses. A batch of 30 g of starting materials thoroughly mixed in agate mortar and the homogeneous mixture was kept in an electric furnace at a temperature of $1100\text{ }^\circ\text{C}$ for 2 h. The molten mixture then poured onto a preheated stainless steel mold at a temperature of $430\text{ }^\circ\text{C}$ until the glass solidifies. Then the glass samples annealed at the same temperature $430\text{ }^\circ\text{C}$ for 10 h

to remove thermal strains and stress. Then the samples were allowed to cool to room temperature. Finally, the prepared glasses were cut and polished for optical measurements.

2.2 Characterization Techniques

The density of the samples was determined by Archimedes' method with water as an immersion liquid. The refractive indices of these glasses were measured using PTR 46X refractometer at 589 nm with the mono-bromonaphthalene as contact layer between the sample and prism of the refractometer. X-ray diffraction (XRD) patterns for the prepared samples recorded with a Philips X-ray diffractometer using mono-chromatized CuK_α radiation of wavelength 1.54056 \AA from a fixed source operated at 45 kV and 9 mA . The morphological studies and compositional analysis were performed using scanning electron microscope (SEM) aided with energy dispersive x-ray QUANTA-FEG250 and operating at 35 kV . Absorption spectra ($200\text{--}1800\text{ nm}$) measured using the spectrophotometer, model V-570 UV/VIS/NIR. The instrument specified by resolution 0.1 nm and wavelength accuracy $\pm 0.3\text{ nm}$ (at a spectral bandwidth of 0.5 nm). The measurements were made on the glass and glass powder, immediately after glass preparation and all spectra measured at room temperature.

3 Results and Discussion

3.1 Physical Properties

Physical properties for the prepared samples such as average molecular weight M_w , density (ρ), molar volume (V_M), concentration of the rare-earth ions (N), and refractive index (n) are shown in Table 1. As the concentration of Yb^{3+} is increased, slight increase in the density and molar volume of the samples is observed. However, no variation in refractive index is witnessed with change in composition.

3.2 Structural Analysis

The XRD patterns of PANBK0.5Er0.5Yb, PANBK0.5Er0.75Yb, and PANBK0.5Er1Yb glasses are shown in Fig. 1. All the glass samples exhibit similar pattern with no sharp diffraction peak

Table 1 The physical properties of PANBK0.5Er0.5Yb, PANBK0.5Er0.75Yb, and PANBK0.5Er1Yb glasses

Sample	Physical properties				
	M_w (gm)	ρ (gm/cm^3)	V_m (cm^3)	N ($\times 10^{+20}$ ions/ cm^3)	n
PANBK0.5Er0.5Yb	133.69	2.811	47.47	1.44198	1.648
PANBK0.5Er0.75Yb	134.19	2.814	47.69	1.43546	1.648
PANBK0.5Er1Yb	134.94	2.817	47.91	1.42902	1.648

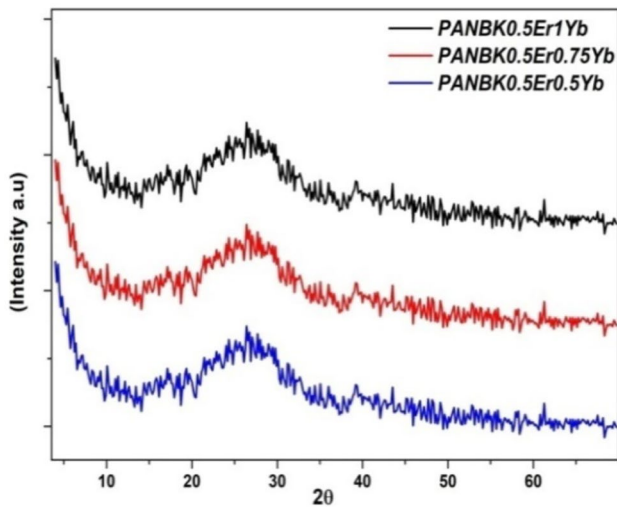


Fig. 1 The XRD patterns of PANBK0.5Er0.5Yb, PANBK0.5Er0.75Yb, and PANBK0.5Er1Yb glasses

but broad humps, which indicates the absence of long-range ordered structure. This is the characteristic of amorphous materials. Hence, all the synthesized glass samples had maintained the amorphous behavior.

3.3 Surface Morphology

Figure 2 shows the morphology of the PANBK0.5Er0.5Yb, PANBK0.5Er0.75Yb, and PANBK0.5Er1Yb glasses captured using FESEM facility. It is evident that the surfaces of the samples are smooth thus confirming the dense glass matrix. Absence of grain boundary indicates the amorphous nature of the samples. This is consistent with the XRD analysis. EDAX analysis performed on the synthesized glass samples in order to qualitatively study the presence of the elements. Figure 3 shows the EDAX spectra of the PANBK0.5Er0.5Yb, PANBK0.5Er0.75Yb, and PANBK0.5Er1Yb glasses. The EDAX spectrum confirms the existence of phosphate, oxygen, aluminum, sodium, potassium, barium, erbium, and ytterbium in the glass matrix.

3.4 Absorption Spectra and J–O Parameters

Figure 4 shows absorption coefficient spectra of PANBK0.5Er0.5Yb, PANBK0.5Er0.75Yb, and PANBK0.5Er1Yb glasses in the region between 300 and 1650 nm. The spectrum consists of 11 bands attributed to the transitions from the ground-state $^4I_{15/2}$ up to the various higher states $^4I_{13/2}$, $^4I_{11/2}$, $^4I_{9/2}$, $^4F_{9/2}$, $^4S_{3/2}$, $^2H_{11/2}$, $^4F_{7/2}$, $^4F_{5/2}$, $^2G_{9/2}$, $^4G_{11/2}$, and $^4G_{9/2}$, respectively. The band around 970 nm is corresponding to $^2F_{7/2} \rightarrow ^2F_{5/2}$ (Yb^{3+}) and $^4I_{11/2} \rightarrow ^4I_{15/2}$ (Er^{3+})

transitions. The absorption bands' presence is due to energy levels reported for Er^{3+} ion glass systems [16, 17]. As seen in Fig. 3, the absorption coefficient around 970 nm increased strongly by increasing the Yb^{3+} ion concentration while the other bands slightly increased. The increase in peak intensities (Fig. 2) confirms that the Yb^{3+} ions act as a sensitizer for the Er^{3+} : Yb^{3+} ions co-activated the multicomponent phosphate system, as previously reported by our team works [18].

The electrostatic $F_{(2)}$, $F_{(4)}$, and $F_{(6)}$ as well as spin–orbit (ζ) parameters were obtained using standard least-square fitting approach technique between calculated barycenter energies and experimental barycenter energies as shown in Table 2 for PANBK0.5Er0.5Yb, PANBK0.5Er0.75Yb, and PANBK0.5Er1Yb glasses [19]. A little bit variation in electrostatic and spin–orbit parameters were noticed which is expected for limited variation of the glass composition. However, Table 3 presents the calculated and experimentally observed energy levels (cm^{-1}) for PANBK0.5Er0.5Yb, PANBK0.5Er0.75Yb, and PANBK0.5Er1Yb glasses. Both the calculation of $F_{(2)}$, $F_{(4)}$, $F_{(6)}$, and ζ parameters (Table 2) and energy levels (Table 3) were carried out using RELEC program [19]. The agreement between experimental and calculated energy indicates the good fitting of the electrostatic spin–orbit (ζ) and ($F_{(2)}$, $F_{(4)}$, $F_{(6)}$) parameters.

The experimental oscillator strengths (f_{exp}) for all the absorption bands of Er^{3+} ions can be determined from the absorption spectra using the expression given by Eq. (1) [20].

$$f_{exp}(\Psi J \rightarrow \Psi' J') = \frac{mc^2}{\pi e^2} \int \epsilon(\nu) d\nu = 4.318 \times 10^{-9} \int \epsilon(\nu) d\nu \tag{1}$$

where m and e are the mass and the charge of an electron, respectively, and c is the speed of light and ν is the wave-number (in cm^{-1}).

According to JO theory, the total oscillator strength can be calculated using Eq. (2).

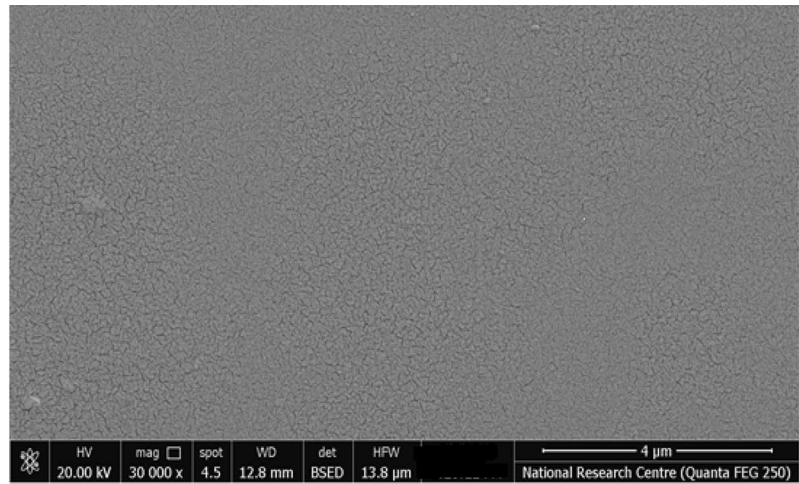
$$f_{calc}(\Psi J \rightarrow \Psi' J') = \frac{8\pi^2 m \nu_0}{3h(2j+1)n^2} [\chi_{ed} S_{ed} + \chi_{md} S_{md}] \tag{2}$$

where S_{ed} and S_{md} are the electric and magnetic dipole line strengths, and $\chi_{ed} = n(n^2 + 2)^2/9$ and $\chi_{md} = n^3$ are the Dexter correction for the local field in a medium of refractive index “ n ”;

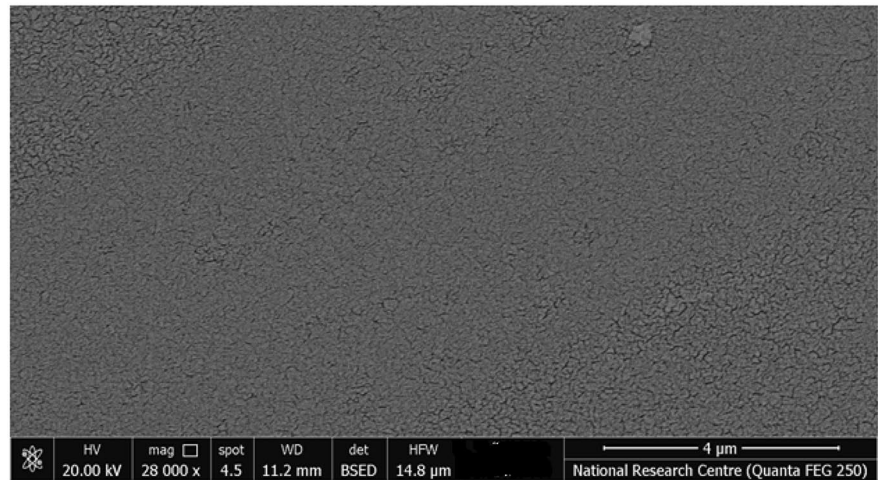
$$S_{ed}(\Psi J \rightarrow \Psi' J') = \frac{8\pi^2 m \nu_0 \chi_{ed}}{3h(2j+1)n^2} \left[\sum_{t=2,4,6} \Omega_t |\langle i || U^t || j \rangle|^2 \right] \tag{3}$$

$$S_{md}(\Psi J \rightarrow \Psi' J') = \frac{e^2 h^2 \chi_{md}}{16\pi^2 m^2 c^2} |\langle i || L + 2S || j \rangle|^2 \tag{4}$$

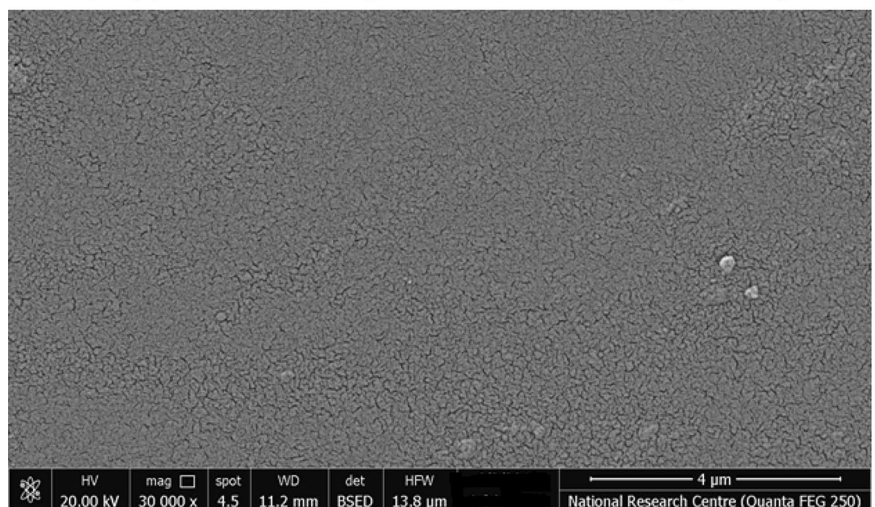
Fig. 2 **a** The FESEM image of PANBK0.5Er0.5Yb glass sample. **b** The FESEM image of PANBK0.5Er0.75Yb glass sample. **c** The FESEM image of PANBK0.5Er1Yb glass sample



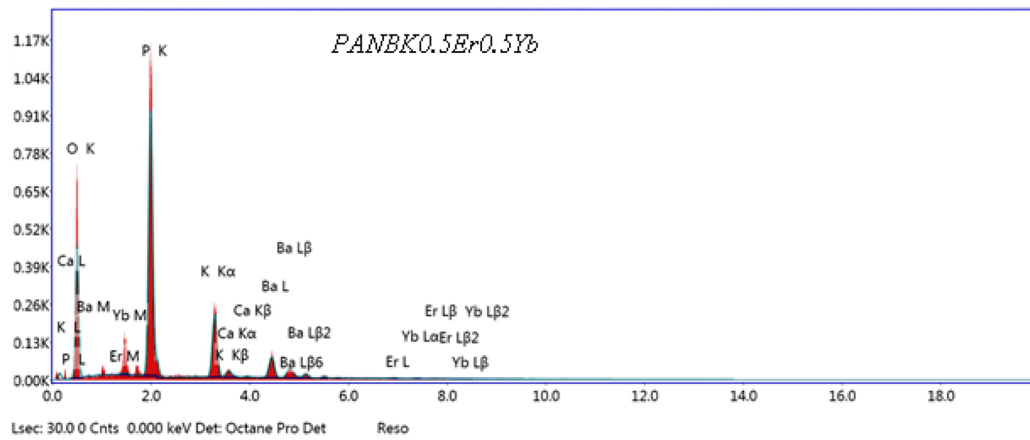
(a) The FESEM image of PANBK0.5Er0.5Yb glass sample



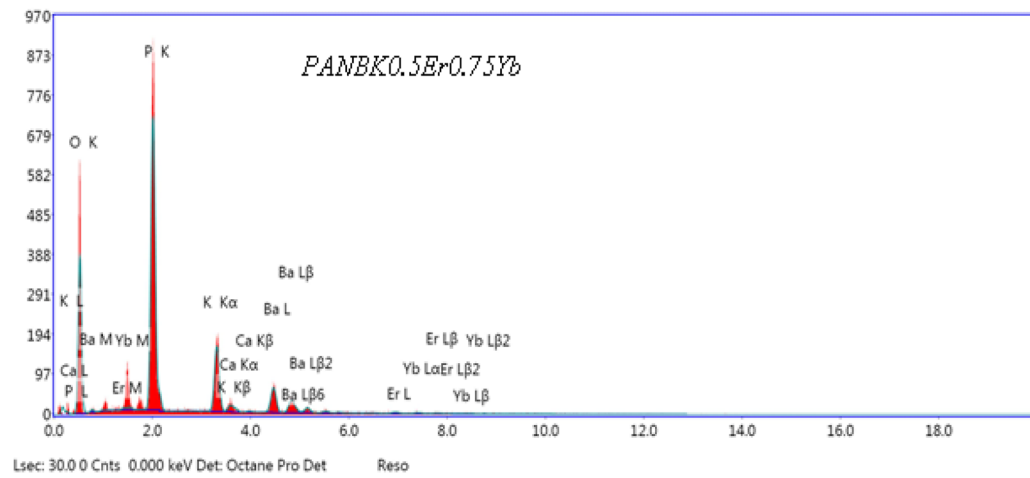
(b) The FESEM image of PANBK0.5Er0.75Yb glass sample



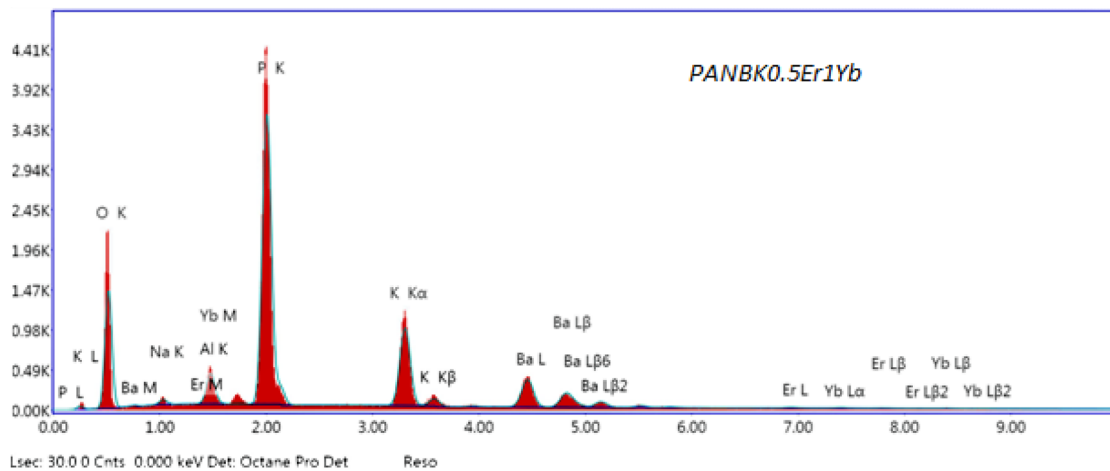
(c) The FESEM image of PANBK0.5Er1Yb glass sample



(a) The EDAX spectra of PANBK0.5Er0.5Yb glass sample



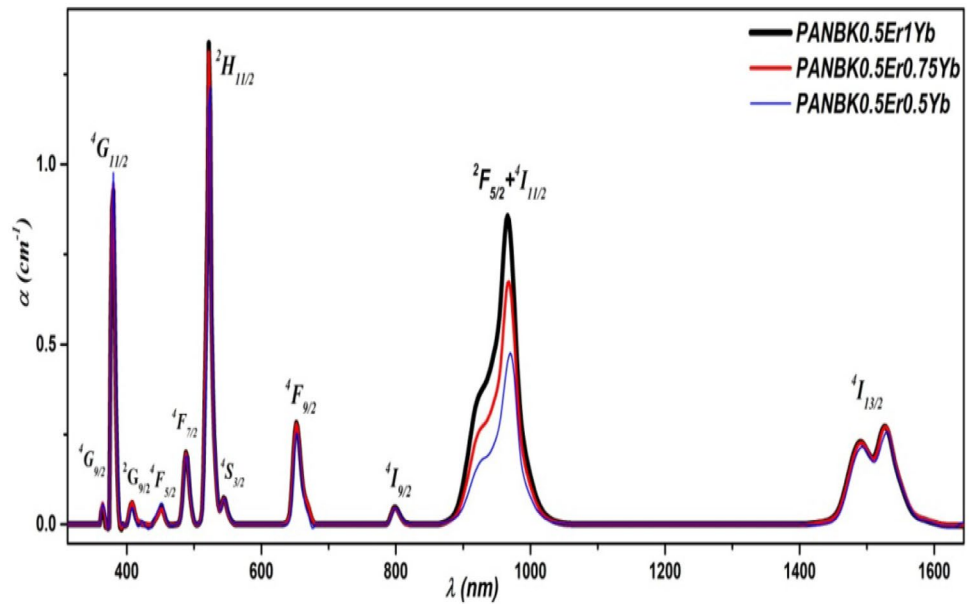
(b) The EDAX spectra of PANBK0.5Er0.75Yb glass sample



(c) The EDAX spectra of PANBK0.5Er1Yb glass sample

Fig. 3 a The EDAX spectra of PANBK0.5Er0.5Yb glass sample, b the EDAX spectra of PANBK0.5Er0.75Yb glass sample, c the EDAX spectra of PANBK0.5Er1Yb glass sample

Fig. 4 The absorption coefficient spectra of PANBK0.5Er0.5Yb, PANBK0.5Er0.75Yb, and PANBK0.5Er1Yb glasses



where Ω_t ($t = 2, 4,$ and 6) are Judd–Ofelt intensity parameters, m is the electron mass, ν_0 is the wavenumber at the absorption maximum (in cm^{-1}), h is the Planck constant $h = 6.6261 \times 10^{-27}$ erg.sec, $2J + 1$ is the degeneracy of the originating level of the transition, and $\langle i || U^t || j \rangle$ are the doubly reduced matrix elements of the tensor transition operator, which were calculated using $F_{(2)}$, $F_{(4)}$, $F_{(6)}$, and ζ parameters.

The Judd–Ofelt intensity parameters Ω_t ($t = 2, 4,$ and 6) can be determined using least-square fitting technique

between experimental (f_{exp}) and calculated (f_{calc}) oscillator strength. Table 4 shows Judd–Ofelt parameters and spectroscopic quality factor ($\chi = \Omega_4/\Omega_6$) for PANBK0.5Er0.5Yb, PANBK0.5Er0.75Yb, and PANBK0.5Er1Yb glasses. All the samples have the same trend ($\Omega_2 > \Omega_6 > \Omega_4$) and spectroscopic factor have maximum value for PANBK0.5Er1Yb sample. Table 5 shows f_{exp} and f_{calc} of PANBK0.5Er0.5Yb, PANBK0.5Er0.75Yb, and PANBK0.5Er1Yb glasses. All the calculations were performed using RELEC program.

Table 2 $F_{(2)}$, $F_{(4)}$, $F_{(6)}$, and ζ parameters for PANBK0.5Er0.5Yb, PANBK0.5Er0.75Yb, and PANBK0.5Er1Yb glasses

Parameters	Glass samples		
	PANBK0.5Er0.5Yb	PANBK0.5Er0.75Yb	PANBK0.5Er1Yb
$F_{(2)}$	434.3	435.9	434
$F_{(4)}$	66.7	66.4	66.8
$F_{(6)}$	7.3	7.3	7.3
ζ	2418.7	2419.7	2420.5

Table 3 Theoretically calculated and experimentally observed energy levels (cm^{-1}) for PANBK0.5Er0.5Yb, PANBK0.5Er0.75Yb, and PANBK0.5Er1Yb glasses

Energy level	Glass samples					
	PANBK0.5Er0.5Yb		PANBK0.5Er0.75Yb		PANBK0.5Er1Yb	
	E_{exp}	E_{calc}	E_{exp}	E_{calc}	E_{exp}	E_{calc}
$^4I_{13/2}$	6611.66	6623.2	6617.18	6626	6621.73	6628.2
$^4I_{9/2}$	12,493.51	12,357.6	12,503.16	12,353.3	12,495.77	12,366.24
$^4F_{9/2}$	15,270.2	15,231.2	15,257.22	15,236.5	15,266.2	15,245.6
$^4S_{3/2}$	18,382.3	18,368	18,382.3	18,384.5	18,382.3	18,380.4
$^2H_{11/2}$	19,106.76	19,258.06	19,132.27	19,237.1	19,134.99	19,265
$^4F_{7/2}$	20,437.32	20,427.5	20,461.46	20,438.2	20,465.23	20,447.7
$^4F_{5/2}$	22,238.4	22,076.8	22,276.72	22,103.2	22,233.53	22,090.2
$^2G_{9/2}$	24,512.31	24,563.6	24,461.38	24,522.5	24,538.17	24,584.9
$^4G_{11/2}$	26,283.75	26,550.3	26,318.4	26,553.5	26,324.57	26,574.1

Table 4 Judd–Ofelt parameters ($\Omega_i \times 10^{20} \text{ cm}^2$), spectroscopic quality factor ($\chi = \Omega_4/\Omega_6$) for PANBK0.5Er0.5Yb, PANBK0.5Er0.75Yb, and PANBK0.5Er1Yb glasses

Host Matrix	Ω_2	Ω_4	Ω_6	$\chi = \Omega_4/\Omega_6$	Trend
PANBK0.5Er0.5Yb	1.68	0.31	0.40	0.775	$\Omega_2 > \Omega_6 > \Omega_4$
PANBK0.5Er0.75Yb	1.76	0.31	0.48	0.646	$\Omega_2 > \Omega_6 > \Omega_4$
PANBK0.5Er1Yb	1.77	0.36	0.45	0.8	$\Omega_2 > \Omega_6 > \Omega_4$

Once the J.O parameters have been obtained, some important radiative parameters can be derived such as the following.

The spontaneous emission probability (A) of an electric-dipole transition is given by the following equation [21]:

$$A_r(\Psi J \rightarrow \Psi' J') = \frac{64\pi^4 \nu_0^2 e^2}{3h(2j+1)} \left[\frac{n(n^2+1)^2}{9} S_{ed} + n^3 S_{md} \right] \quad (5)$$

where S_{ed} and S_{md} are the electric and magnetic dipole line strengths respectively which are expressed as

$$S_{ed}(\Psi J \rightarrow \Psi' J') = \sum_{t=2,4,6} \Omega_t \left| \langle J || U^t || J' \rangle \right|^2 \quad (6)$$

$$S_{md}(\Psi J \rightarrow \Psi' J') = \frac{h^2}{16\pi^2 m^2 c^2} \left| \langle J || L + 2S || J' \rangle \right|^2 \quad (7)$$

The total radiative transition probability $A_r(\Psi J)$ for an excited level is given by the sum of the $A(\Psi J \rightarrow \Psi' J')$ terms calculated over all terminal levels [21, 22].

$$A_r(\Psi J) = \sum A(\Psi J \rightarrow \Psi' J') \quad (8)$$

The fluorescence branching ratio B_r has been determined using

$$B_r = \frac{A(\Psi J \rightarrow \Psi' J')}{A_r(\Psi J)} \quad (9)$$

Table 5 Experimental and calculated oscillator strengths for PANBK0.5Er0.5Yb, PANBK0.5Er0.75Yb, and PANBK0.5Er1Yb glasses

Transition from the ground state $^4I_{15/2}$ to	Glass samples					
	PANBK0.5Er0.5Yb		PANBK0.5Er0.75Yb		PANBK0.5Er1Yb	
	f_{exp}	f_{calc}	f_{exp}	f_{calc}	f_{exp}	f_{calc}
$^4I_{13/2}$	0.62	0.95	0.67	1.03	0.68	1.01
$^4I_{9/2}$	0.08	0.08	0.08	0.08	0.09	0.10
$^4F_{9/2}$	0.7	0.54	0.86	0.59	0.85	0.61
$^4S_{3/2}$	0.32	0.17	0.26	0.2	0.34	0.19
$^2H_{11/2}$	3.08	2.69	3.36	2.81	3.45	2.85
$^4F_{7/2}$	0.68	0.62	0.69	0.72	0.71	0.70
$^4F_{5/2}$	0.38	0.2	0.26	0.24	0.26	0.23
$^2G_{9/2}$	0.19	0.24	0.30	0.29	0.25	0.28
$^4G_{11/2}$	4.29	4.64	4.40	4.86	4.44	4.94

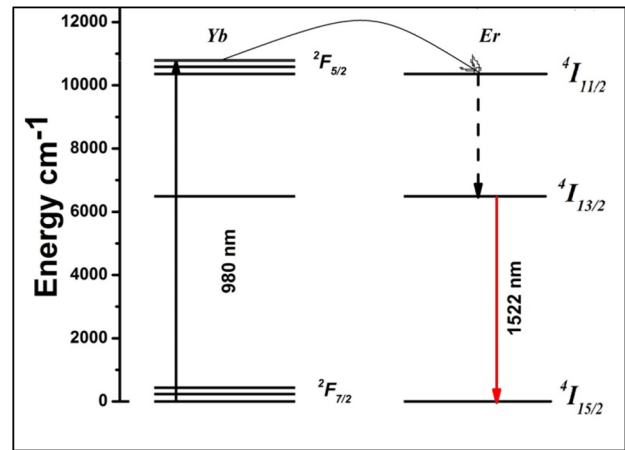


Fig. 5 Partial energy level diagram of the Er³⁺ and Yb³⁺ ions showing the energy transfer process and NIR emission mechanism

The radiative lifetime $\tau_r(\Psi J)$ of an excited level (ΨJ) is given by the reciprocal of $A_r(\Psi J)$.

$$\tau_r(\Psi J) = \frac{1}{A_r(\Psi J)} \quad (10)$$

The Yb³⁺ and Er³⁺ ions have a highly overlapped levels, where after the 980-nm laser pumping, both Yb³⁺ and Er³⁺ ions are resonantly excited from their ground states to the highly overlapped $^2F_{5/2}$ (Yb³⁺) and $^4I_{11/2}$ (Er³⁺), respectively. The absorption probability of the Yb³⁺ ion is at least one order of magnitude bigger and wider than that of the Er³⁺ ion. As seen in Fig. 5, a part of Yb³⁺ ion nonradiative energy transfer to Er³⁺ ion works on promoting the population of $^4I_{11/2}$ level. The $^4I_{11/2}$ level de-excites non-radiatively to $^4I_{13/2}$ level. The $^4I_{13/2}$ level is a Meta stable level and a population inversion can happen with $^4I_{15/2}$ level.

The spectroscopic radiative properties of $^4I_{13/2}$ level for PANBK0.5Er0.5Yb, PANBK0.5Er0.75Yb, and PANBK0.5Er1Yb compared with other glasses reported earlier are presented in Table 6. Comparatively, greater enhancement

Table 6 Radiative transition probability (A), total transition probability (A_T), radiative lifetime (τ_r), and branching ratio (B_r) for the excited ${}^4I_{13/2}$ of PANBK0.5Er0.5Yb, PANBK0.5Er0.75Yb, and PANBK0.5Er1Yb glasses

Glass samples	Parameters		
	B_r	A_T (s^{-1})	τ_r (ms)
PANBK0.5Er0.5Yb	1	87	11.49
PANBK0.5Er0.75Yb	1	93.77	10.66
PANBK0.5Er1Yb	1	92.3	10.83
NZLE2 [22]	1	117.92	8.48
PBNEY2 [23]	1	497.5	2.201

in τ_r has been observed for the glasses under study. The value of τ_r is found to differ slightly with change in Yb^{3+} ion concentration [6–8, 23]. Data obtained were compared with the earlier published results and were found to be consistent.

3.5 Photoluminescence Study

Figure 6 illustrates the photoluminescence (PL) spectra of (a) PANBK0.5Er0.5Yb, (b) PANBK0.5Er0.75Yb, and (c) PANBK0.5Er1Yb glasses, excited at 980 nm. The emission intensity is found to increase with an increase of Yb^{3+} ion concentration up to 0.75 mol%, while a quenching phenomenon in phosphate prepared sample at higher content of 1 mol% of ytterbium ion concentration is examined. For as-melted phosphate, (c) PANBK0.5Er1Yb sample the PL lifetime decreases. This decrease is attributed to a combined concentration quenching process depending on both rare

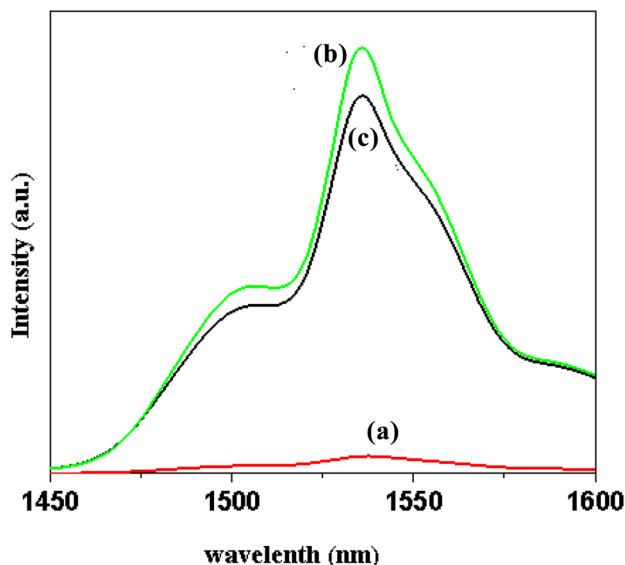


Fig. 6 (PL) spectra of **a** PANBK0.5Er0.5Yb, **b** PANBK0.5Er0.75Yb, and **c** PANBK0.5Er1Yb glasses excited at 980 nm

earth ($0.5Er^{3+}:1Yb^{3+}$) and the OH level in the melting glass [24–26]. It is clear that the emission band profiles are not modified by the 1 mol% of Yb^{3+} ion concentration. Thus, it can be concluded that the Yb^{3+} ions being homogeneously distributed in the glass matrix and no variation in the local crystal field around dopant ions would be felt. This illustrates the negligible chance of physical clustering; however, higher Yb^{3+} ions dopant concentration may lead to luminescence quenching due to the cross relaxation. In addition, higher intensity photoluminescence band emission at about 1.5- μm results for the prepared sample doped with 0.5 mol% Er^{3+} and 0.75 mol% Yb^{3+} may be used in the future to support single-mode planar optical waveguide optical sensor application. In fact, it is well known that the most important needed factors for supporting planar optical wave-guide sensor application are the higher thickness, higher transparency observed in Fig. 4, which shows the absorption coefficient spectra of PANBK0.5Er0.5Yb, PANBK0.5Er0.75Yb, and PANBK0.5Er1Yb glasses and higher refractive indices at $n = 1.648$, Table 1, of the prepared samples as well as the PL results in the NIR region at 1.5 μm leading to PANBK0.5Er0.75Yb sample to support wave-guide optical sensor system application.

4 Conclusion

Er^{3+} - Yb^{3+} co-activated Na–Al–Ba–K phosphate glasses were prepared by conventional melt quenching technique. XRD examination reveals that all the samples were in amorphous phase. FE-SEM images confirmed the homogeneous, very dense nature, and smooth surface of the samples. The absorption spectra analyzed using the Judd–Ofelt theory. The τ_r slightly decrease changes with the increase in Yb^{3+} ion sensitizer, and it has maximum value (11.49 ms) for PANBK0.5Er0.5Yb sample. The photoluminescence (PL) emission spectra indicate that the addition of Yb^{3+} ions enhanced the emission intensity of the glasses at 0.75 mol% Yb, while a quenching phenomenon is examined at 1 mol% of ytterbium ion concentration, due to the combined concentration quenching process depending on both rare earth ($0.5Er^{3+}:1Yb^{3+}$) and the OH level in the melting glass. These results obviously indicate that the prepared glasses are suitable for laser as well as wave-guide optical sensor and amplifiers applications at $\approx 1.5 \mu m$. Hence, 0.5 mol% Er^{3+} –0.75 mol% Yb^{3+} ion co-activated multicomponent phosphate prepared samples can be considered promising material for advanced new laser communication and photonic applications. It is well known that the most important needed factors for supporting planar optical wave-guide sensor application are the higher thickness, higher transparency, and higher refractive indices at $n = 1.648$ and the PL results in the NIR region at 1.5 μm present with the higher intensity

in PANBK0.5Er0.75Yb sample supports wave-guide optical sensor system applications.

Acknowledgements The co-authors acknowledge Dr. D. Atta, Spectroscopy Department, Physics Research Institute, National Research Centre, for his help in (PL) measurement.

Funding This work is supported financially by the Indo-Egyptian Joint project Fund, entitled, Investigations on the physical and optical performances of Er³⁺/Yb³⁺ co-doped silica-phosphate glasses to develop high-gain laser materials with enhanced wave-guide optical applications (2020–2022), code-number (M.H. No.1.126.).

Declarations

Competing Interests The authors declare no competing interests.

References

1. T. Okura, Y. Nojima, K. Kawada, Y. Kojima, K. Yamashita, *Ceram. Int.* **47**, 1940 (2021)
2. L. Cognolato, A. Gnazzo, *Opt. Mater.* **2**, 1 (1993)
3. J. Wang, B. Zheng, P. Wang, *J. Non-Crys. Solids.* **530**, 120362 (2020)
4. Z. Chen, Y. Wang, R. Lv, S. Liu, J. Wang, Y. Wang, *Opt. Fiber Tech.* **58**, 102189 (2020)
5. Y.H. Lu, S. Chi, *Opt. Commn.* **229**, 317 (2004)
6. Y. Badr, I.K. Battisha, A. Salah, M.A. Salem, *Indian J. Pure Appl. Phy.* **46**, 706 (2008)
7. I.K. Battisha, *J. Non-Cryst. Solids.* **353**, 1748 (2007)
8. I.K. Battisha, Y. Badr, N.M. Shash, M.G. El –Shaarawy, A.G.A. Darwish, *J. Solgel Sci. Technol.* **53**, 543 (2010)
9. F. Auzel, *Chem. Rev.* **104**, 139 (2004)
10. F. Rivera-López, P. Babu, L. Jyothi, U.R. Rodríguez-Mendoza, I.R. Martín, C.K. Jayasankar et al., *Optical Mater.* **34**, 1235 (2012)
11. H. Lin, E.Y.B. Pun, S.Q. Man, X.R. Liu *J. Opt. Soc. Am. B.* **18**, 602 (2001)
12. J. Pisarska, *J. Non-Crys. Solids.* **345**, 382 (2004)
13. J.H. Campbell, T.I. Suratwala, *J. Non-Crys. Solids.* **263**, 318 (2000)
14. S. Tian, Y. Lun, Y. Sun, G. Tang, Q. Qian, Z. Yang, *J. Non-Crys. Solids.* **577**, 121313 (2022)
15. F. Rivera-López, P. Babu, Ch. Basavapoornima, C.K. Jayasankar, V. Lavín *J. Appl. Phys.* **109**, 123514 (2011)
16. C.C. Santos, I. Guedes, C.K. Loong, L.A. Boatner, A.L. Moura, M. Td. Araujo, *PhyD: Appl. Phys.* **43**, 02510 (2009)
17. A.A. Reddy, S.S. Babu, K. Pradeesh, C.J. Otton, G.V. Prakash, *Alloy Compd.* **509**, 4047 (2011)
18. A. Amin, E.H. Ahmed, C. Wickleder, M. Adlung, A.I. Hashem, M.H. Ayoub et al., *J. Polym. Compos.* **2029** (2019)
19. M.M. Ismail, H. Farouk, M.A. Salem, A. Ashery, I.K. Battisha, *J. Scientific Res. Sci.* **36469** (2019)
20. M.M. Ismail, I.K. Battisha, L. Zur, A. Chiasera, M. Ferrari, A. Lukowiak, *J. Optical Mater.* **99**, 109591 (2020)
21. M.J. Weber, *J. Phys. Rev.* **157**, 262 (1967)
22. D.E. McCumber, *J. Phy. Rev.* **134 b**, A954 (1964)
23. A. Langar, C. Bouzidi, H. Elhouichet, M. Férid, *Luminescence* **148**, 249 (2014)
24. E.H. Ahmed, M.M. Magdy A.I. Hashem, I.K. Battisha, C. Wickleder, M. Adlung et al., *J. Polymer-Plastics Tech. Eng.* **60**, 744 (2021)
25. E.H. Ahmed, M.M.H. Ayoub, A.I. Hashem, C. Wickleder, M. Adlung, A. Amin et al., *Thin Film. Inter. J. Photochem. Photobiol.* **5**, 28 (2021)
26. D. Atta, M.M. Ismail, I.K. Battisha, *J. Optics Laser Tech.* in press (2021)

Publisher's Note Springer Nature remains neutral with regard to jurisdictional claims in published maps and institutional affiliations.

Springer Nature or its licensor (e.g. a society or other partner) holds exclusive rights to this article under a publishing agreement with the author(s) or other rightsholder(s); author self-archiving of the accepted manuscript version of this article is solely governed by the terms of such publishing agreement and applicable law.